

The influence of nitrogen to hydrogen ratio and temperature on thickness and phase composition in plasma nitrided Ti-6Al-4V

Saulo Cordeiro Lima¹, Ruth Hinrichs²,
Marcos Antonio Zen Vasconcellos³

¹ Programa de Pós-Graduação em Física (PPGFIS), Universidade Federal do Rio Grande do Sul, Porto Alegre, Rio Grande do Sul, Brasil.

² Instituto de Geociências, Universidade Federal do Rio Grande do Sul, Porto Alegre, Rio Grande do Sul, Brasil.

³ Instituto de Física, Universidade Federal do Rio Grande do Sul, Porto Alegre, Rio Grande do Sul, Brasil.

e-mail: saulocl@gmail.com, ruth.hinrichs@ufrgs.br, marcos@if.ufrgs.br

ABSTRACT

Ti-6Al-4V was plasma nitrided using several N₂/H₂ ratios and substrate temperatures. In order to investigate the combined influence of these parameters on phase composition and thickness of the coatings, the phases in the as received, annealed, and nitrided Ti-6Al-4V samples were identified with Rietveld refinement. In the as-received and annealed samples the structure parameters of α -Ti and β -Ti were slightly changed, due to the substitution of titanium atoms by Al or V in the α - and β -Ti unit cells. A combination of multiple angle grazing incidence X-ray diffraction, nuclear reaction analysis and cross sectional micrographs showed compound layers consisting of an outer layer of stoichiometric δ -TiN over a phase mixture of δ -TiN and ϵ -Ti₂N, formed on top of a nitrogen diffusion region in the alloy. Higher nitriding temperatures induced thicker compound layers, and higher nitrogen content of the plasma induced thicker fine-grained δ -TiN top layers.

Keywords: plasma nitriding, Ti-6Al-4V, titanium nitride, Rietveld analysis.

1. INTRODUCTION

The most widely used titanium alloy, Ti-6Al-4V, has an excellent combination of strength, toughness, and corrosion resistance [1] and is applied in aircraft-turbines, pressure vessels, compressor blades [2], and in biomedical applications [3]. However, due to its low hardness, wear resistance is poor and surface coatings are used to improve it.

Nitrides of titanium are very hard and can be reactively formed on the sample surface by plasma nitriding, establishing a hardness gradient that helps to prevent cracking of the coating under load [4]. Plasma nitriding at high temperature promotes the formation of ultra-hard δ -TiN (3000 HV) and the formation of thick layers [5-11], however above 850 °C the fatigue properties of Ti-6Al-4V degrade due to grain growth [12]. To obtain ϵ -Ti₂N, which has intermediate hardness (1500 HV), lower nitriding temperatures are more appropriate.

In plasma nitriding several process parameters affect the phases that are formed in the coating, such as substrate temperature, gas composition, gas pressure, gas flow, voltage, current, current density, and deposition time. The influence of atmosphere (N₂/H₂ ratio) on compound layer thickness and phase composition has been investigated before in selected ranges, but only a couple authors worked in the range below 800 °C, varying gas composition. SILVA et al. [6] used 20% and 60% N₂ in N₂+H₂, varying temperature between 400 °C and 670 °C. They conclude that at temperatures below 500 °C, ϵ -Ti₂N and δ -TiN are present only in samples nitrided in 60% N₂ atmosphere. CHEN and JAUNG [8] tested several temperatures with one gas composition (75 % N₂), and several gas compositions at 800 °C, and concluded that the thickest layers (at 800°C) were obtained with 82.5% N₂. BRADING et al. [7] used a wide compositional range of N₂ in N₂+H₂ at 700 °C, however their substrate was commercially pure titanium. Surprisingly they observed the thickest TiN layers on samples nitrided in atmospheres with less than 30% N₂.

So, with the intent of discriminating the influence of the atmosphere on phase formation and thickness of the coatings, in this work we characterized Ti-6Al-4V samples that were plasma nitrided in 5 different N₂/H₂ ratios at 500 °C, 600 °C, and 700 °C. The as received and annealed Ti-6Al-4V samples were character-

ized with Rietveld analysis to establish the modification of the substrate phases with heat treatment. Using different incidence angles in grazing incidence X-ray diffraction (multiple angle MA-GIXRD) allowed the discrimination of phases in different depths. Nuclear reaction analysis (NRA) provided nitrogen depth profiles. The thickness of the compound layer was determined on cross sections, machined into the surface layer with a focused ion beam (FIB).

2. MATERIALS AND METHODS

2.1 Sample preparation

Ti-6Al-4V discs of 10 mm diameter and 3 mm thickness (Goodfellow, nominal composition see Table 1) were metallographically polished, degreased in an ultrasonic acetone bath, rinsed with deionized water, and dried.

Table 1: Nominal composition of the Ti-6Al-4V substrate, in wt%

Al	V	O	N	Fe	C	H	Ti
5.97	3.9	0.12	0.09	0.09	0.014	0.027	balance

Before the nitriding process, the samples were plasma etched in argon (1 kPa, 500 °C) for 30 minutes and consecutively pumped to base pressure (3 Pa), before establishing temperature and dynamic pressure (1.3 kPa) in the desired N₂/H₂ gas mixture (flow rate of 20 sccm). Table 2 presents the voltages and currents necessary to obtain the target temperatures in different atmospheres. After 4 hours of plasma treatment, samples were cooled in the chamber without oxygen admission.

Table 2: Voltages and currents necessary to obtain the target temperatures in different atmospheres.

Atmosphere	700 °C		600 °C		500 °C	
	Voltage (V)	Current (mA)	Voltage (V)	Current (mA)	Voltage (V)	Current (mA)
80N ₂ /20H ₂	415	172	348	140	318	96
60N ₂ /40H ₂	447	136	388	114	341	100
50N ₂ /50H ₂	480	148	415	131	363	111
40N ₂ /60H ₂	502	133	434	122	386	93
20N ₂ /80H ₂	*	*	502	110	436	84

*no voltage/current combination resulted in stable 700 °C with this gas composition

2.2 Phase analysis with Rietveld refinement of broad range X-ray diffraction scans

Rietveld analyses of broad range XRD scans (D8 Advance, Bruker AXS) were performed to determine crystal structure of as received, annealed, and nitrided samples of the Ti-6Al-4V. Phases were identified using information from the Inorganic Crystal Structure Database (ICSD) and the PDF cards of the International Center of Diffraction Data (ICDD®).

2.3 Depth characterization with multiple-angle grazing incidence X-ray diffraction

In MA-GIXRD the incidence angle of the X-ray beam on the sample surface determines the effective diffraction depth. In order to analyze consecutively deeper layers, five diffractograms were obtained per sample, using incidence angles of 0.5°, 1°, 2°, 4°, and 6° (XRD6000, Shimadzu). The approximate diffraction depths, calculated [13] for the mass absorption coefficient of TiN, are presented in Table 3.

Table 3: Approximate thickness of the layers that generate 95% of the diffraction peak intensity at different incidence angles in GIXRD of titanium nitrides.

Incidence angle (°)	0.5	1	2	4	6
Depth (µm)	0.3	0.6	1.1	2.1	3.1

2.4 Characterization with nuclear reaction analysis

The depth distribution of nitrogen in the outermost 200-nm-layers of the samples was determined with nuclear reaction analysis (NRA) in a 500 kV linear particle accelerator (High Voltage Engineering Europe - HVEE). When protons of 429 keV hit a nitrogen atom, they can produce the nuclear reaction $^{15}\text{N}(p,\alpha\gamma)^{12}\text{C}$ and the presence of nitrogen can be determined measuring the characteristic 4.43 MeV γ -ray. The nitrogen depth profile can be determined varying the proton energy from 429 to 455 keV. Calibration was performed with a standard of Si_3N_4 , presuming a natural abundance of 0.37% of the ^{15}N isotope [14].

2.5 Imaging with Ga-ion induced secondary electrons

In order to image the cross-section of the nitrided layers, ten-micrometer wide trenches were machined into the surface using 30 keV Ga-ions in a focused ion beam (SEM-FIB, Jeol JIB4500). Secondary electron images induced by Ga-ions (Ga-SEI) were obtained from the polished wall.

3. RESULTS AND DISCUSSION

3.1 Phase identification using Rietveld refinement

Fig. 1 compares the diffractogram and the Rietveld refinement of the as received and the annealed Ti-6Al-4V samples. The Rietveld adjustment was started with the unit cell parameter values of pure Ti (α and β phases). To account for the alloying elements, Al atoms were allowed to substitute Ti in the hexagonal close-packed (hcp) structure of α -Ti, with space group P63/mmc, and V atoms in the body centered cubic (bcc) structure of β -Ti with space group Im3m. All peaks were accounted using α -Ti and β -Ti structures.

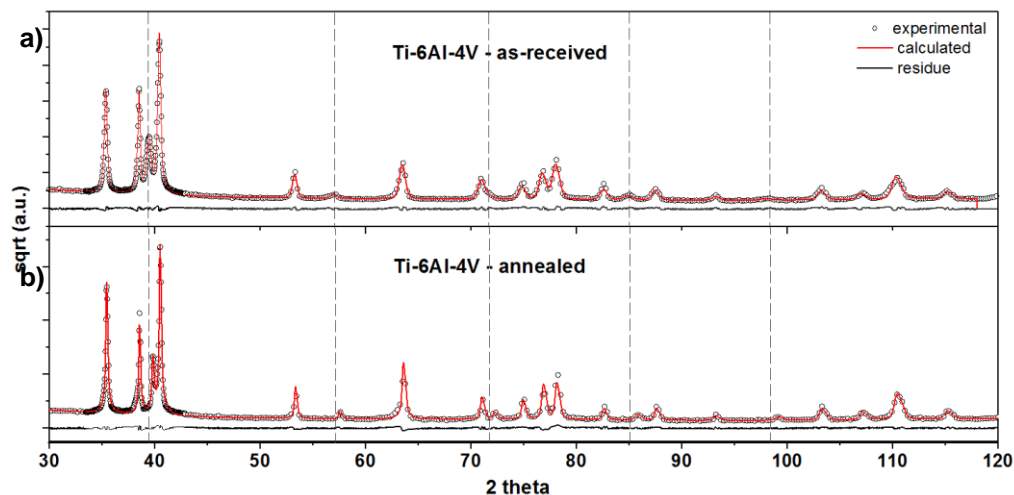


Figure 1: XRD patterns from a) as received and b) annealed Ti-6Al-4V. The experimental points are shown as circles, the two phase Rietveld refinement as light grey line, the difference between them (residue) as black line. The vertical dashed lines indicate the positions of β -Ti(V)-peaks of the as received sample.

Due to the incorporation of β -stabilizing V, in the as received Ti-6Al-4V the β -phase presented a cell parameter that was 2.5 % smaller than the one indicated in the literature (PDF card 44-1288). After annealing, the cell parameter decreased even more (additional 0.8 %), however the peaks were consistent with the bcc structure of the β -phase, from now on designated β -Ti(V). All other peaks were consistent with the hexagonal α -Ti, presenting cell parameter changes smaller than 1 % compared to the PDF card, or else compatible

with α' -Ti-martensite, which has the same structure and almost the same unit cell parameters as α -Ti [20], and is discriminated from the latter mainly by metallographic texture arguments. This structure was detected as well in the nitrated samples and is henceforth designated α -Ti(Al). In the as received Ti-6Al-4V, the peaks were broader than the in the annealed samples and might point to α' -martensite. After annealing, all phases showed narrower peaks, implying larger grain size and higher cristallinity. Unit cell parameters and peak widths before and after annealing are presented in Table 4.

Table 4: Sample identification, phases, structures, fitting parameters (Rietveld), card numbers and cell parameters from the Powder Diffraction File (PDF), and fitted FWHM of the α - and β -Ti (011) peaks.

Sample ID	phase	structure	fitting parameters	PDF card numbers	PDF parameters	FWHM $d_{(011)}$
Titanium (pure)	α -Ti	$P6_3/mmc$	a=2.9500 c=4.6860	44-1294	a=2.9505 c=4.6826	
as-recieved Ti-6Al-4V	α -Ti(Al)	$P6_3/mmc$	a=2.9266 c=4.6683	44-1294	a=2.9505 c=4.6826	0.28°
	β -Ti(V)	$Im3m$	a=3.2257	44-1288	a=3.3065	0.39°
annealed Ti-6Al-4V	α -Ti(Al)	$P6_3/mmc$	a=2.9258 c=4.6708	44-1294	a=2.9505 c=4.6826	0.20°
	β -Ti(V)	$Im3m$	a=3.2016	44-1288	a=3.3065	0.23°
nitrated Ti-6Al-4V	α -Ti(Al)	$P6_3/mmc$	a=2.9225 c=4.6828	44-1294	a=2.9505 c=4.6826	
	β -Ti(V)	$Im3m$	a=3.1814	44-1288	a=3.3065	
	δ -TiN	$Fm-3m$	a=4.2294	38-1420	a=4.2417	
	ϵ -Ti ₂ N	$P4_2/mnm$	a=4.9436 c=3.0286	76-0198	a=4.9452 c=3.0342	

In Fig. 2 the Rietveld refinement of a GIXRD pattern of Ti-6Al-4V nitrated at 600 °C, 80N₂/20H₂ is used to exemplify the quality of the adjustment using four phases (β -Ti(V), α -Ti(Al), δ -TiN and ϵ -Ti₂N). The experimental pattern overlaps well with the calculated sum. The calculated patterns of the individual phases, shifted for clarity, are shown below the experimental diffractogram. The refinement showed that the cell parameters of α -Ti(Al) changed less than 0.3 % and β -Ti(V) changed 0.6 % compared to the values obtained in the annealed Ti-6Al-4V. The changes of cell parameters of the nitrated phases were within 0.3 % when compared to the PDF-cards (Table 4). The crystallographic structures of the phases were stable, the fit converged within the whole range, and the residue shows that all peaks are accounted for.

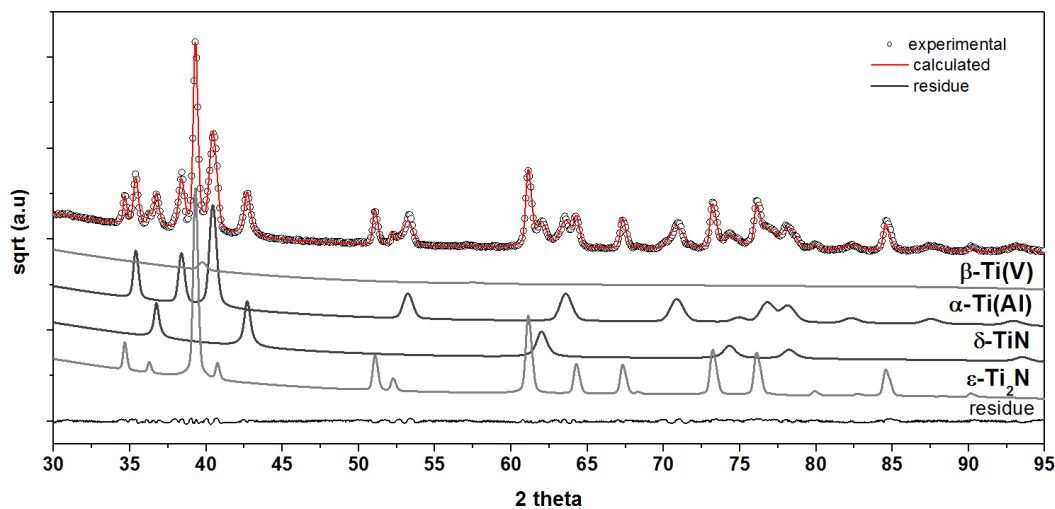


Figure 2: GIXRD of plasma-nitrated Ti-6Al-4V (600 °C, 80N₂/20H₂) and Rietveld refinement using α -Ti(Al), β -Ti(V), δ -TiN, and ϵ -Ti₂N (individual traces shifted for clarity). Residue shows the difference between experimental and calculated points.

The presence of δ -TiN and ε -Ti₂N on nitrated Ti-6Al-4V has long been described in the literature [5-12, 15, 16], however the unambiguous peak assignment of nitrated phases on titanium is not straightforward, due to severe peak overlaps in the range that is mostly used for identification (33° to 45°). Our interpretation is based on Rietveld refinement of a much broader range (30° to 95°), where the phases δ -TiN, ε -Ti₂N, α -Ti(Al), and β -Ti(V) account for all peaks.

3.2 Depth distribution of phases with MA-GIXRD

MA-GIXRD patterns were evaluated in the range from 33° to 45°, which contains strong peaks of all phases that were identified in the broad scan. Fig. 3 shows the MA-GIXRD patterns from the Ti-6Al-4V samples treated in 80N₂/20H₂ atmospheres, at all three temperatures, stacked according to incidence angle.

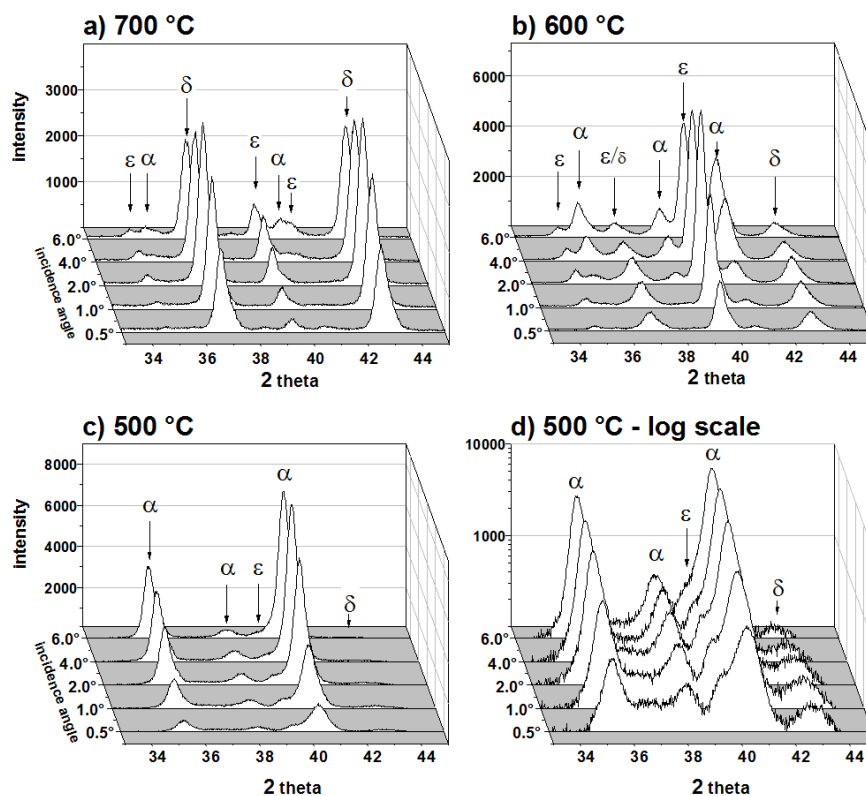


Figure 3: MA-GIXRD from Ti-6Al-4V samples, nitrated in 80N₂/20H₂ atmosphere at: a) 700 °C, b) 600 °C, and c) 500 °C; d) repeats 500 °C in log scale, with emphasis on the very small δ -TiN peak.

In MA-GIXRD the peak intensities initially rise with increasing incidence angle, until the gain in diffraction volume is counterbalanced by higher X-ray absorption in the exit path and the peak intensity saturates. In bulk Ti-6Al-4V, this saturation is observed at incidence angles around 6°. In layered structures the incidence angle indicates the depth where a phase starts to appear. When the peak rises to a maximum and then decreases, the incidence angle after the maximum encompasses a depth where the phase no longer exists, therefore revealing the stacking order of the phases.

In Fig. 3a (700 °C), the most intense δ -TiN peak increases until a maximum at 2°, whereas the peaks of ε -Ti₂N reach their highest intensity at 4°. This peak intensity evolution evidences a layered structure, with δ -TiN on top of ε -Ti₂N. The α -Ti peak appears only at incidence angles above 4°, implying that this phase enters the diffraction volume only at depths greater than 2 μ m.

In Fig. 3b (600 °C) ε -Ti₂N peaks are most intense at 2° incidence angle. δ -TiN peaks present the same intensity for 1° and 2° incidence angles. The α -Ti peak from the substrate appears at 2°, indicating that this phase is present at depths > 1 μ m.

Fig. 3c (500 °C) shows intense peaks from the substrate already at 0.5°, revealing the small thickness of the nitrated layer. The δ -TiN and ε -Ti₂N peaks are only discernible in the log scale graph (Fig. 3d). The

observation of an incipient compound layer at 500 °C extends the nitride formation range to lower temperatures then suggested by Chen [8], who had established a threshold temperature of 600 °C for the formation of ϵ -Ti₂N, and 700 °C for δ -TiN.

3.3 Influence of atmosphere on phases

In order to assess the effects of gas mixture on the depth distribution of the phases, the 1° GIXRD patterns (depth ~ 0.6 μ m) of all samples were analyzed and are shown in Fig. 4, stacked according to increasing nitrogen concentration in the plasma.

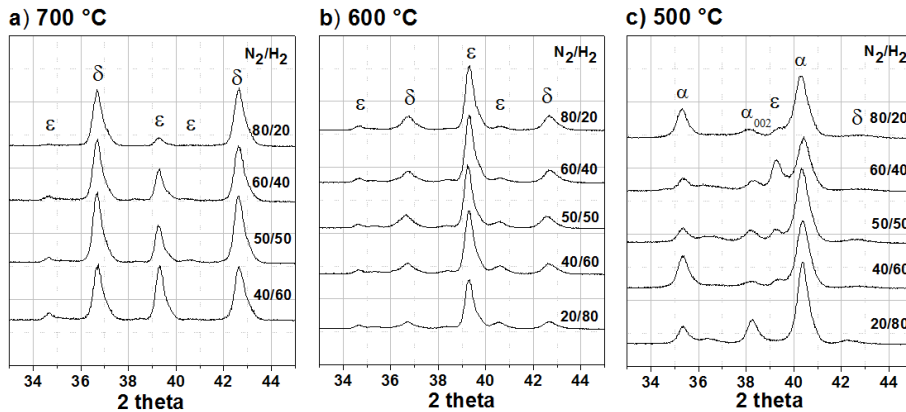


Figure 4: 1° GIXRD patterns of Ti-6Al-4V treated at: a) 700 °C, b) 600 °C, and c) 500 °C ; N₂/H₂ ratios are indicated at the right hand side of each pattern.

The diffractograms of the samples nitrided at 700 °C and 600 °C (Figs. 4a and 4b) show the presence of δ -Ti and ϵ -Ti₂N, forming a compound layer thick enough (> 0.6 μ m) to block the peaks from the substrate. At 700 °C (Fig. 4a), the δ -TiN peak dominates all patterns and the relative intensity of the ϵ -Ti₂N peak decreases with rising nitrogen concentration in the gas mixture. We interpret this as evidence that the outermost δ -TiN layers with increasing thickness block the ϵ -Ti₂N diffraction peak from the layer below. At 600 °C (Fig. 4b) the intensity of the δ -TiN peak increases with rising nitrogen content, but is always lower than the ϵ -Ti₂N peak. At 500 °C (Fig. 4c), only small amounts of δ -TiN and ϵ -Ti₂N were formed, and the peaks from the substrate are always observed, revealing that the compound layer on the surface was thinner than 0.6 μ m for all gas compositions.

3.4 Elemental analysis with NRA

The NRA results in Fig. 5 show the nitrogen profiles from the surface to a depth of 200 nm, a region even shallower than the one examined with the lowest incidence angle in GIXRD.

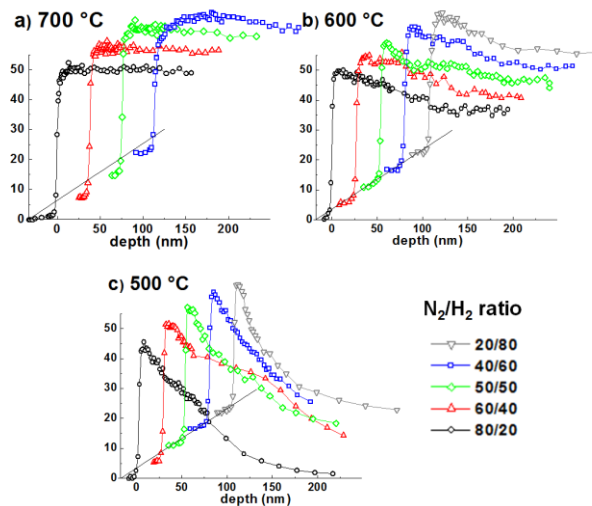


Figure 5: Nitrogen depth profiles in the Ti-6Al-4V nitrided at a) 700 °C, b) 600 °C, and c) 500 °C ; N₂/H₂ ratios are indicated.

In all the samples nitrided at 700 °C (Fig. 5a) the nitrogen content reached 50 at% (stoichiometric δ -TiN) in the whole range probed with NRA. In Fig. 5b (600 °C) δ -TiN was only observed at small depths, falling to a plateau of ~33 at% (ϵ -Ti₂N). At 500 °C (Fig. 5c) δ -TiN formed at depths < 5 nm, than the nitrogen distribution decreased smoothly without the formation of plateaus, except at the gas mixture of 60N₂/40H₂, where a small ~33 at% plateau formed, and at 80N₂/20H₂, where the surface seems to have lost some nitrogen in favor of an incipient ϵ -Ti₂N plateau.

3.5 Focused Ion Beam imaging of the cross-sectioned nitrided layers

In order to allow direct observation of the layered structure, cross sections were prepared by machining micrometric trenches into the surface of all nitrided samples using the FIB. The Ga-SEI micrographs obtained on the cross sections are shown in Fig. 6. The images present a channeling contrast, depending on crystal orientation of the grains. Vertical stripes on some of the images are artifacts of the FIB machining.

In Fig. 6a (700 °C), a layer of 0.3 μ m to 0.5 μ m thickness of fine-grained material can be seen at the top (indicated with black arrows), with larger grains below, and the grains of the apparently unaltered alloy can be seen at the bottom of each image. In the samples nitrided at 600 °C (Fig. 6b), the altered layers are much thinner, and only at high nitrogen concentrations fine-grained layers can be clearly differentiated on top. At 500 °C (Fig. 6c), hardly any layer can be seen at the surface. Only at 60N₂/40H₂ a thin continuous film is visible, while at the other gas mixtures solely patches of altered material can be discriminated.

The phase identification of the layers seen in the images can be performed by combining the results from Rietveld analysis, MA-GIXRD, and NRA. The upper fine-grained layer of all Ti-6Al-4V samples nitrided at 700 °C is δ -TiN, because NRA showed that nitrogen concentration was 50 at%. The observation of a small α -Ti peak at 4°-GIXRD (not shown) is compatible with the thickness (2-3 μ m) of the nitrided layer observed at 700 °C. The highest δ -TiN peak was found in 2°-GIXRD, indicating that δ -TiN was present in a layer shallower than 1 μ m. In the images, the fine-grained layer is only 0.5 μ m thick, indicating that δ -TiN possibly extends to the lower layer. The peak related to ϵ -Ti₂N increases up to 4°, coming from a layer of ~2 μ m.

At 600 °C, the thickest top layer is observed for the plasma with 80N₂/20H₂. In MA-GIXRD the maximum peak intensity for δ -TiN is observed for incidence angles between 1° and 2°, which points to a depth ~ 0.8 μ m. The peak intensity from ϵ -Ti₂N shows the highest value at 2° incidence angle, which is compatible with a layer thickness of around 1 μ m. So, the larger grains in the second layer seem to be a mixture of δ -TiN and ϵ -Ti₂N. This interpretation is reinforced by the NRA results in Fig. 5b, which show a smooth transition from the stoichiometric δ -TiN to the underlying ϵ -Ti₂N.

At 500 °C, NRA indicated a very thin δ -TiN film on top of the samples, which could barely be identified with GIXRD. The nitrogen content decreased with increasing depth in all samples and only in 80N₂/20H₂ and 60N₂/40H₂ atmospheres, plateaus compatible with ϵ -Ti₂N developed, whereas the diffusion zones showed amounts of nitrogen consistent with a solid solution of nitrogen in titanium.

Extending these analyses to all compound layers, it can be assumed that the phase mixture of the second layer is richer in δ -TiN near the surface and richer in ϵ -Ti₂N at higher depths. A model of thick compound layers obtained with RF-plasma [17] proposed the formation of a δ -TiN layer on top of a ϵ -Ti₂N layer. In our much thinner films we found a structure similar to the one described by [18, 19]: an outer δ -TiN layer, on top of a phase mixture of δ -TiN and ϵ -Ti₂N that gets impoverished in δ -TiN progressively until it consists of ϵ -Ti₂N only, followed by a solid solution of nitrogen in α -Ti. An intermediary layer containing a mixture of phases δ -TiN and ϵ -Ti₂N is compatible with the simplified model by ZHECHEVA et al. [20], using reaction diffusion rules to describe the formation and growth of nitrided layers during gas nitriding of titanium.

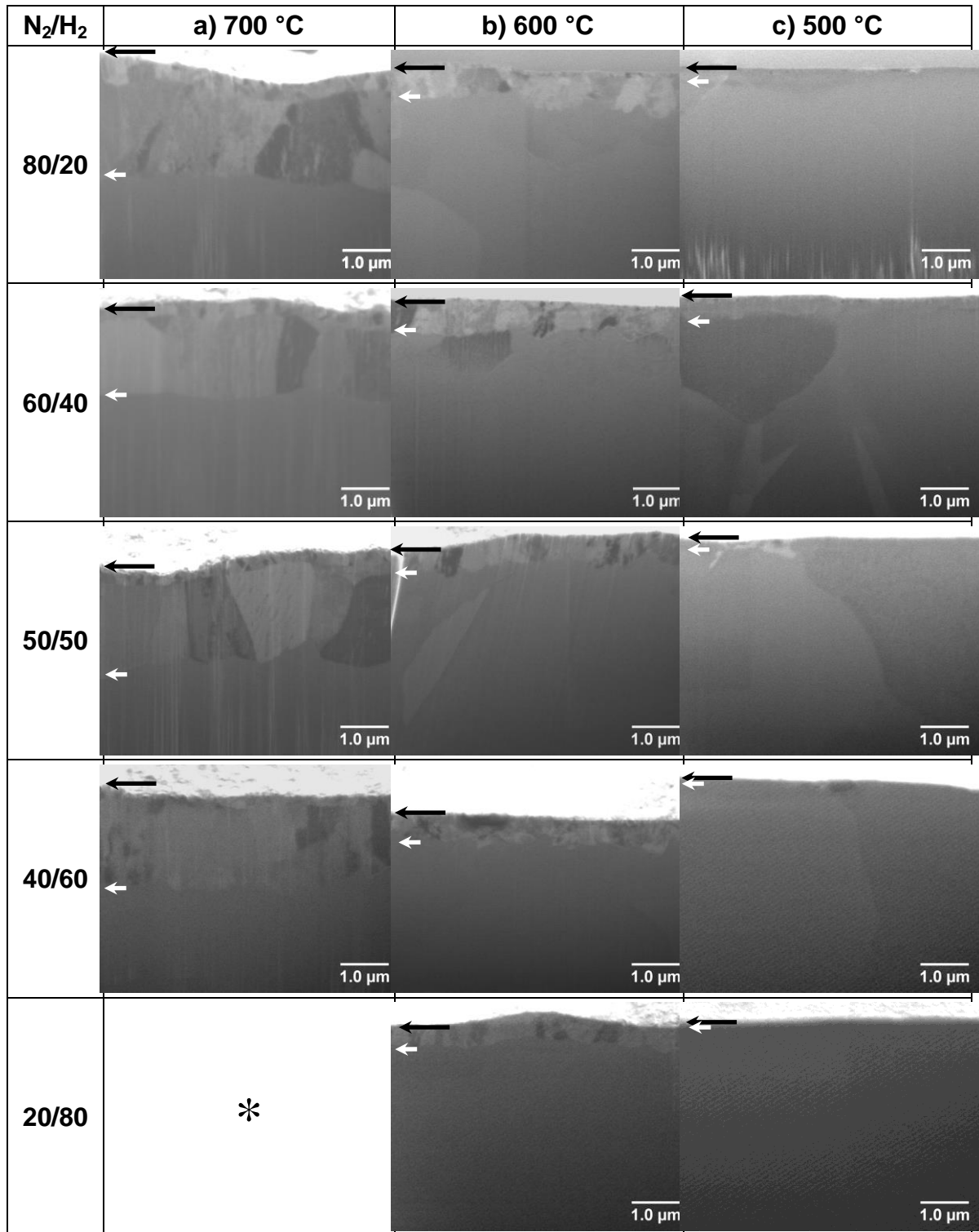


Figure 6: Ga-ion induced secondary electron micrographs of the cross sections of the Ti-6Al-4V samples, nitrided at: a) 700 °C, b) 600 °C, and c) 500 °C. N_2/H_2 ratios are indicated in the first column. The black arrows indicate the top surface and the white arrows indicate the interface between nitrided layers and the substrate. (* no stable plasma was achieved).

Fig. 7 shows a bar graph of layer thickness, measured on the cross sections depicted on the Ga-SEI micrographs of Fig. 6.

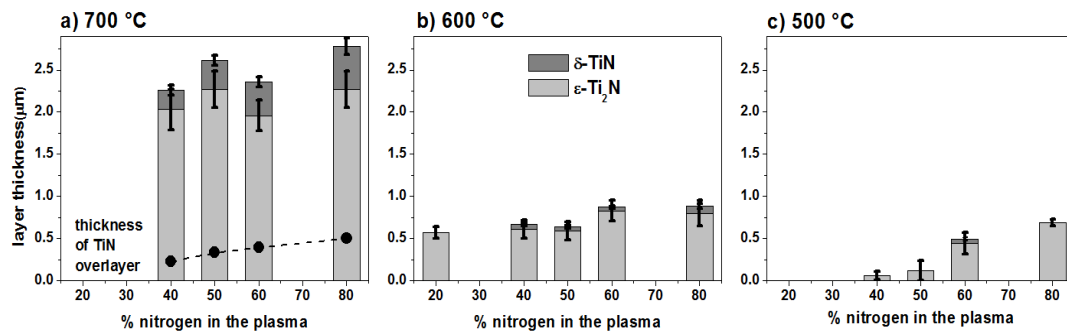


Figure 7: Thickness of the compound layers as a function of nitrogen content in the plasma, discriminating the δ -TiN over layer and the ϵ -Ti₂N + δ -TiN second layer at a) 700 °C, b) 600 °C, and c) 500 °C. In a), the δ -TiN overlayer thickness is repeated with filled symbols, to show the thickness increase with higher nitrogen content in the plasma. Uncertainty was determined with 20 measurements.

Fig. 7a shows the thickness increase (depicted as closed circles) of the outermost δ -TiN layer, obtained in the plasma at 700 °C, as a function of increasing nitrogen concentration, even though the overall thickness of the compound layer is constant within uncertainty. This can be due to the ϵ -Ti₂N phase acting as a diffusion barrier to the nitrogen atoms, as has been pointed out by YILDIZ et al. [10].

The overall thickness increase with temperature of the compound layer can be attributed to the higher ion currents, necessary to establish higher temperatures [7]. As a consequence, more ions reach the surface with enough energy to promote the growth of the nitrated layer.

4. CONCLUSIONS

Rietveld refinement of the as received and annealed Ti-6Al-4V samples showed that, within experimental sensitivity of the XRD, only α -Ti and β -Ti were present, however with modified unit cell parameters due to the incorporation of Al and V.

The plasma nitriding in a broad range of N₂/H₂ gas compositions, at temperatures between 500 °C and 700 °C resulted in :

- i) a double compound layer, consisting an outermost fine grained δ -TiN layer and of a coarse grained second layer, mainly of ϵ -Ti₂N, but containing a fraction of δ -TiN next to the upper interface;
- ii) the compound layer was located on top of a solid solution of nitrogen in titanium, with decreasing nitrogen content towards the bulk;
- iii) at a given temperature, the overall thickness of the compound layer within measurement uncertainty was the same in all atmospheres;
- iv) at each temperature, the major effect of a richer-in-nitrogen atmosphere was to increase the thickness of the δ -TiN top layer.

5. ACKNOWLEDGEMENTS

The authors acknowledge financial support from the Brazilian funding agencies CAPES, CNPq and FAPERGS.

6. BIBLIOGRAPHY

- [1] REVATHI, A., MAGESH, S., BALLA, V.M., et al., "Current advances in enhancement of wear and corrosion resistance of titanium alloys – a review", *Materials Technology*, v. 31, n. 12, pp. 696-704, Aug. 2016.
- [2] PETERS M., HEMPTENMACHER J., KUMPFERT J., et al., "Structure and Properties of Titanium and Titanium Alloys", In: Leyens C, Peters M, (eds), *Titanium and Titanium Alloys. Fundamentals and Applications*. 1 ed., chapter 1. Weinheim, Germany, Wiley, 2003.

- [3] GUERRA NETO, C.L.B., SILVA, M.A.M., ALVES, C., “Experimental study of plasma nitriding dental implant surfaces”, *Surface Engineering*. v. 25, n. 6, pp. 430-433, Jul. 2009.
- [4] HOSSEINI, S.R., AHMADI, A., “Characterisation of the structure and the tribological behaviour of PN/PVD duplex processed Ti6Al4V”, *Surface Engineering*. v. 33, n. 1, pp. 27-34, Dec. 2016.
- [5] BADINI, C., GIANOGLIO, C., BACCI, T., *et al.*, “Characterization of surface layers in ion-nitrided titanium and titanium alloys”, *Journal of the Less-Common Metals*. v. 143, pp. 129-141, Oct. 1988.
- [6] SILVA, S.L.R., KERBER, L.O., AMARAL, L., *et al.*, “X-ray diffraction measurements of plasma-nitrided Ti-6Al-4V”, *Surface and Coating Technology*, v. 116-119, pp. 342-346. Sep. 1999.
- [7] BRADING, H.J., MORTON, P.H., BELL, T., *et al.*, “Plasma nitriding with nitrogen, hydrogen, and argon gas mixtures: structure and composition of coatings on titanium”, *Surface Engineering*. v. 8, n. 3, pp. 206-212, May 1992.
- [8] CHEN K.C., JAUNG G.J., “D.C. diode ion nitriding behavior of titanium and Ti-6Al-4V”, *Thin Solid Films*, v. 303, pp 226-231, Jun. 1997.
- [9] SOUZA, G.B., FOERSTER, C.E., SILVA, S.L.R., *et al.*, “Hardness and elastic modulus of ion-nitrided titanium obtained by nanoindentation”, *Surface and Coating Technology*, v. 191, n. 1, pp 76-82, Feb. 2005.
- [10] YILDIZ, F., YETIM, A.F., ALSARAN, A., *et al.*, “Plasma nitriding behavior of Ti-6Al-4V orthopedic alloy”, *Surface and Coating Technology*, v. 202, n. 11, pp 2471-2476, Feb. 2008.
- [11] HOSSEINI S.R., AHMADI A., “Evaluation of the effects of plasma nitriding temperature and time on the characterisation of Ti 6Al 4V alloy”, *Vacuum*. v. 87, pp. 30-39, Jan. 2013.
- [12] ALI, M.M., RAMAN, S.G.S., PATHAK, S.D., *et al.*, “Influence of plasma nitriding on fretting wear behaviour of Ti-6Al-4V”, *Tribology International*, v. 43, n. 1-2, pp. 152-160, Jan. 2010.
- [13] CULLITY, B.D., STOCK, S.R., *Elements of X-ray Diffraction*. 3rd ed., Harlow, United Kingdom, Pearson, 2014.
- [14] VANAMURTHY, L.H., HABERL, A.W., BAKHRU, H., “Application of ion beams in the study of depth profiling of nitrogen”, *Nuclear Instruments and Methods in Physics Research B*. v. 261, n. 1-2, pp. 516-519, Aug. 2007.
- [15] FOUQUET, V., PICHON, L., DROUET, M., *et al.*, “Plasma assisted nitridation of Ti-6Al-4V”, *Applied Surface Science*. v. 221, n. 1-4, pp. 248-258, Jan. 2004.
- [16] VASCONCELLOS, M.A.Z., LIMA, S.C., HINRICHS, R., “Hardness evaluation, stoichiometry and grain size of titanium nitride films obtained with plasma nitriding on Ti-6Al-4V samples”, *Matéria (R.J.)*, v. 15, n. 2, pp. 299-302, 2010.
- [17] RAAIF, M., EL-HOSSARY, F.M., NEGM, N.Z., *et al.*, “Surface treatment of Ti-6Al-4V alloy by rf plasma nitriding”, *Journal of Physics: Condensed Matter*. v. 39, n. 396003, pp. 1-12. Oct. 2007.
- [18] GRILL, A., RAVEH, A., AVNI, R., “Layer structure and mechanical properties of low pressure R.F. plasma nitrided Ti-6Al-4V Alloy”, *Surface and Coating Technology*, v. 43-44, pp. 745-755, 1990.
- [19] RAVEH, A., BUSSIBA, A., BETTELHEIM, A, *et al.*, “Plasma-nitrided α - β Ti alloy: layer characterization and mechanical properties modification”, *Surface and Coating Technology*. v. 57, pp. 19-29, 1993.
- [20] ZHECHEVA, A, SHA, W., MALINOV, S., *et al.*, “Enhancing the microstructure and properties of titanium alloys through nitriding and other surface engineering methods”, *Surface and Coating Technology*. v. 200, n. 7, pp. 2192-2207, Dec. 2005.

ORCID

Saulo Cordeiro Lima <https://orcid.org/0000-0002-6964-6489>

Ruth Hinrichs <https://orcid.org/0000-0003-0553-0935>

Marcos Antonio Zen Vasconcellos <http://orcid.org/0000-0001-7714-0878>